

The unimolecular dissociation of the OH stretching states of HOCl: Comparison with experimental data

J. Weiß, J. Hauschildt, and R. Schinke

Max-Planck-Institut für Strömungsforschung, D-37073 Göttingen, Germany

O. Haan

Gesellschaft für Wissenschaftliche Datenverarbeitung Göttingen, D-37077 Göttingen, Germany

S. Skokov and J. M. Bowman

Department of Chemistry and Cherry L. Emerson Center for Scientific Computation, Emory University, Atlanta, Georgia 30322

V. A. Mandelshtam

Chemistry Department, University of California, Irvine, California 92697

K. A. Peterson

Department of Chemistry, Washington State University and Environmental Molecular Science Laboratory, Pacific Northwest National Laboratory, Richland, Washington 99352

(Received 19 July 2001; accepted 29 August 2001)

The unimolecular dissociation of the $(v_1,0,0)$ pure OH stretching states of hypochlorous acid (HOCl) in the ground electronic state is investigated for $v_1=6-9$. The dynamics calculations are performed on an accurate potential energy surface and employ filter diagonalization in connection with an imaginary absorbing potential. The dependence of the linewidth (or dissociation rate) on the total angular momentum is emphasized. Resonance enhancements due to mixings with other vibrational states, which have substantially larger rates, are clearly observed—in *qualitative* agreement with recent measurements. The average width increases, in *quantitative* agreement with experiments, by four orders of magnitude, from 10^{-4} cm^{-1} for $v_1=6$ to about 1 cm^{-1} for $v_1=9$.

© 2001 American Institute of Physics. [DOI: 10.1063/1.1412602]

I. INTRODUCTION

Hypochlorous acid, HOCl, is a prototype system for investigating bond breaking on ground-state potential energy surfaces (PES) without reaction barriers and has been the subject of intense research in the past few years (see Refs. 1–4, and references therein). Because of the relatively weak intramolecular coupling between the HO stretch (mode ν_1) on the one hand, and the OCl stretch (mode ν_3) and the bending mode (ν_2), on the other hand, the dynamics is remarkably regular, even at energies around the HO+Cl dissociation limit.^{5,6} As a consequence, the pure HO stretching states $(v_1,0,0)$ (the “bright” states) have simple wave functions and good Franck–Condon overlaps with the vibrational ground state, and therefore can be selectively excited by overtone pumping.

The rotationless state $(6,0,0)$ is bound by $\sim 160 \text{ cm}^{-1}$. However, rotational excitation of the parent molecule lifts its energy above the dissociation threshold and ultimately enables breaking of the O–Cl bond. The dissociative lifetime, $\tau(J,K)$, depends on the amount of rotational excitation, where J is the rotational angular momentum quantum number and K is the projection quantum number of \mathbf{J} on the body-fixed a -axis, which is essentially the O–Cl axis. Since the vibrational-rotational coupling is exceedingly weak, the lifetimes of the highly excited $(6,0,0|J,K)$ states are very long, in the range of 10^{-9} – 10^{-6} s .^{2,3}

Using overtone–overtone double resonance spectros-

copy Callegari *et al.*² and Dutton *et al.*³ were able to measure the decay rate, $k(J,K)=1/\tau$, of state $(6,0,0)$ for many rotational quantum numbers J and K . The main observation is the large fluctuation of $k(J,K)$ by up to two orders of magnitude as a function of J . These fluctuations are ascribed to—mainly accidental—mixing of the “bright” state $(6,0,0)$ with nearby “dark” states $(v_1 < 6, v_2, v_3)$. The vibrational state dependence of the rotational constants causes the “bright” state to tune in and out of “resonance” with energetically close “dark” states as J is varied.

Recently, the experimental investigations have been extended by Callegari *et al.*⁴ up to $v_1=8$. The main observations are: First, the average rate increases by about two orders of magnitude from $v_1=6$ to 7 and again by two orders of magnitude from $v_1=7$ to 8. Second, the fluctuations, when J is varied, are considerably smaller than for $v_1=6$; for $v_1=8$ rather clear resonancelike maxima are observed.

HOCl is small enough to allow a rigorous theoretical investigation and the experimental data of Callegari *et al.*^{2,4} and Dutton *et al.*³ provide excellent ground for testing the ability of state-of-the-art quantum dynamics calculations. High-level global *ab initio* PES, including all three internal degrees of freedom, have been determined by two groups.^{6–9} These potential energy surfaces subsequently have been used in two sets of dynamics calculations. Both sets exploited imaginary absorbing potentials; however, different numerical methods for obtaining the complex eigenstate energies, from which the decay widths are determined, have been em-

ployed. While Bowman and co-workers^{10–12} used a truncation/recoupling (TR) scheme, which is global in energy, Schinke and co-workers^{6,13,14} calculated the resonance energies by means of the filter diagonalization (FD) method.^{15–17} The FD method is in practice more accurate, because the set of basis functions used for diagonalizing the Hamiltonian are adapted for a particular energy window; thus, the dimension of the Hamiltonian matrix to be diagonalized is small. Storing the basis function, which is necessary for calculating after the diagonalization the eigenfunctions, may require a large memory. If that is the case, the energy window can be made very narrow so that only a manageable number of basis functions suffices. In the TR approach, on the other hand, energy independent basis functions are employed and therefore a rapidly increasing number of functions are required for converging the results at high energies; the dimension of the Hamiltonian matrix quickly becomes too large for a direct diagonalization.

Both sets of calculations gave only fair (order of magnitude) agreement with the experimental rate constants for (6,0,0), the only data available at that time; finer details were not satisfactorily reproduced. Because of the smallness of the resonance widths, the results are extremely sensitive to inaccuracies of both the PES and the numerical procedures. The PES used in the calculations of Hauschildt *et al.*¹⁴ slightly overestimates the dissociation energy with the result that actually more rotational quanta are required to lift state (6,0,0) above the threshold than in reality. In addition, the level structure of the experimentally known vibrational states, especially in the region of (6,0,0), is not reproduced with the required precision. The PES employed by Skokov and Bowman¹² is more accurate in this respect.

In the present study we describe calculations, which combine the best of each venture: the PES of the Bowman group, further improved by a perturbative inversion approach,⁹ and the FD method for solving the Schrödinger equation. It will be shown, that the gross features, i.e., the J -averaged rates and the tremendous increase of the rate from $v_1=6$ to 8 by about four orders of magnitude are quantitatively reproduced. The resonancelike features due to coupling with nearby dark states are only qualitatively described; the calculations reproduce them, but not always at the correct J values.

II. DYNAMICS CALCULATIONS

The dynamics calculations in the present study employ the version of the FD method of Refs. 17 and 18. In the first step a set of optimal, energy-window adapted basis functions Ψ_i is generated by applying the Green's function $\hat{G}^+(E_i) = (E_i - \hat{H} + iW)^{-1}$ with $E_{\min} \leq E_i \leq E_{\max}$ as a filtering operator onto an initial wave packet χ , where iW represents a complex absorbing potential. The filtering is done by expanding the Green's operator in damped Chebyshev polynomials,¹⁶ which is an extension of approaches described in Refs. 19–21, that did not implement damping. In the second step, the spectral information in the small energy window $[E_{\min}, E_{\max}]$ is extracted by diagonalizing the full Hamiltonian in the basis $\{\Psi_i\}$. The FD method has the ad-

vantage that the eigenenergies and corresponding wave functions can be fully converged, irrespective of the energy range studied. The downside is, that many energy windows have to be considered in order to sample a larger energy range. However, in the present investigation we solely concentrate on the vicinity of one and only one particular vibrational-rotational state, $(v_1, 0, 0 | J, K=0)$, and the energy window can be chosen to be very small.

The discrete variable representation is employed for representing the wave functions. As in previous calculations,¹⁴ we adopt the following grids: $2.5 a_0 \leq R \leq 14.0 a_0$ with 220 potential optimized points,²² $1.0 a_0 \leq r \leq 3.5 a_0$ with 30 potential optimized points, and 70 Gauss–Legendre quadrature points²³ in the interval $0 \leq \gamma \leq 180^\circ$. Here, R is the distance from Cl to the center-of-mass of HO, r is the HO separation, and γ is the corresponding Jacobi angle with $\gamma=180^\circ$ corresponding to linear HOCl. All points with energies exceeding a certain limit E_{lim} are discarded from the grid: $E_{\text{lim}} = 2$ eV for (6,0,0) and 2.4 eV for the other calculations. Energy is measured with respect to $\text{OH}(r_e) + \text{Cl}$. The large number of grid points in R accounts for the fact, that the heavy Cl atom is split off. The form of the optical potential iW is explicitly given in Refs. 6 and 16. It contains two parameters, R_{damp} , the distance at which the complex potential is switched on, and D_0 , the strength of this potential. In the present study, R_{damp} is chosen to be $12 a_0$ and D_0 is taken as 0.1 (Ref. 14).

Lifting state (6,0,0) above the dissociation threshold requires a large amount of rotational energy. For example, the first open state for $K=0$ has $J=18$ and the range studied experimentally extends to $J=30$. The high degree of rotational excitation poses a severe numerical problem, because exact calculations, in which all K -blocks from $K=0$ through $K=J$ are included, are prohibitively large for the size of grid described above. (K is the quantum number for the projection of the total angular momentum vector on \mathbf{R} ; R -embedding.) In the present study we consider only states with $K=0$, and therefore it should suffice to take into account a limited number of K -blocks from $K=0$ to K_{max} . In Ref. 14 we checked the convergence with respect to K_{max} for $J=25$ and found that the inclusion of three blocks ($K_{\text{max}}=2$) converged the energy of state (6,0,0) within 0.2 cm^{-1} ; increasing K_{max} by one led to an energy change of only 0.01 cm^{-1} . Because of its smallness, the dissociation rate $k(J, K)$ is more difficult to converge with respect to K_{max} . Comparing the results for $K_{\text{max}}=2$ and 3, it was concluded, that the rate is converged within a factor of 2 for $K_{\text{max}}=2$. Nevertheless, restricting the number of K -blocks in the calculations is a severe source of error. In all calculations for $v_1=6$ discussed below $K_{\text{max}}=2$ is used. The calculations for the higher OH stretching quantum numbers, $v_1=7-9$, use only the $K=0$ block for reasons to be discussed below.

Including more K -blocks drastically increases the computer time. First, the number of floating point operations grows linearly with K_{max} . Second, the density of states grows linearly with each additional K manifold and as a consequence the number of Chebyshev iterations also has to grow. For example, if three K values are included, about 400 000 iterations have to be performed in order to establish

TABLE I. Calculated resonance energies E , resonance widths Γ , and dissociation rates k for vibrational states (6,0,0) and (4,4,2).

J	(6,0,0)			(4,4,2)		
	E^a	Γ	k	E	Γ	k
19	19 311.63	1.0(-5) ^b	1.9 (0)	19 319.57	1.7(-3)	3.2 (2)
20	19 331.34	5.6(-6)	1.0 (0)	19 338.68	2.2(-2)	4.1 (3)
21	19 352.02	2.3(-4)	4.3 (1)	19 358.80	4.2(-2)	7.9 (3)
22	19 373.69	4.3(-4)	8.1 (1)	19 379.79	1.5(-2)	2.8 (3)
23	19 396.33	5.7(-6)	1.1 (0)	19 402.13	2.9(-3)	5.5 (3)
24	19 419.95	1.9(-4)	3.6 (1)	19 423.81	9.8(-3)	1.8 (3)
25	19 444.54	3.0(-4)	5.6 (1)	19 446.63	7.9(-3)	1.5 (3)
26	19 470.10	1.8(-3)	3.4 (2)	19 470.12 ^c	2.2(-3)	4.1 (2)
27	19 496.64	5.6(-4)	1.0 (2)	19 499.59	1.8(-2)	3.4 (3)
28	19 524.13	4.8(-4)	9.0 (1)	19 526.07 ^c	1.1(-1)	2.1 (4)

^aEnergies and widths in cm^{-1} , rates in μs^{-1} . The energies are measured with respect to (0,0,0) and $J=0$.

^bNumbers in parentheses indicate powers of 10.

^cThe (4,4,2) state is strongly mixed with another state.

an appropriate basis, compared to 180 000 iterations when Coriolis coupling is not taken into account.

All calculations are done on a CRAY T3E parallel computer including 16 CPUs and using Message Passing Interface (MPI) software. The basis functions Ψ_i constructed by applying the Green's operator to an initial wave function are equally distributed among the 16 CPUs. This allows one to store all functions in the core memory. In order to achieve a significant speed up in CPU time, the multiplication of the Hamiltonian matrix with the Chebycheff vector is distributed among the processors so that each processor has to perform roughly the same number of floating point operations. For 16 processors a speed-up factor of nearly 10 is achieved.

III. RESULTS

A. State (6,0,0)

We will first discuss the calculations for state (6,0,0), which are the most extensive ones. They are performed for $J=19$ –28 using energy windows with $\Delta E \approx 50 \text{ cm}^{-1}$. Reasonable windows can be chosen by extrapolation from J to $J+1$ using the rotational constant for the (6,0,0) state. The calculated value is $\bar{B}=0.493 \text{ cm}^{-1}$ as determined from the energies for $J=19$ and 20. The experimental¹ value is 0.495 cm^{-1} . Since the density of states is high, it is essential to visually inspect the wave function in order to identify the correct state.

The energies, resonance widths Γ , and corresponding dissociation rates k are summarized in Table I and the rates are separately shown in the lower panel of Fig. 1 in comparison to the experimental values. The energy of the rotationally excited state (6,0,0) is barely above threshold. This and the generally weak coupling of the pure OH overtone states to the dissociation mode, causes the bond rupture to be exceedingly slow. The large fluctuations over more than two orders of magnitude result from energy “resonances,” i.e., mixings with near-by (“dark”) states, which have considerably larger dissociation rate constants; this was first noted by Skokov and Bowman in Ref. 12. As a consequence of the quite different structures of their wave functions, the various vibrational states have different rotational constants \bar{B} , which is

approximately associated with rotation of the OCl entity about its center-of-mass. Therefore, as J is varied the energy separations between neighboring states varies also. Because the degree of mixing between different (zero-order) states depends strongly on their energy separation, it is not surprising to find, that the width of a particular state fluctuates strongly with J . The fluctuations due to interactions with other states are obviously most severe for states having a very small rate anyhow. If the rate is larger, the influence of coupling with another state becomes, in relative terms, less

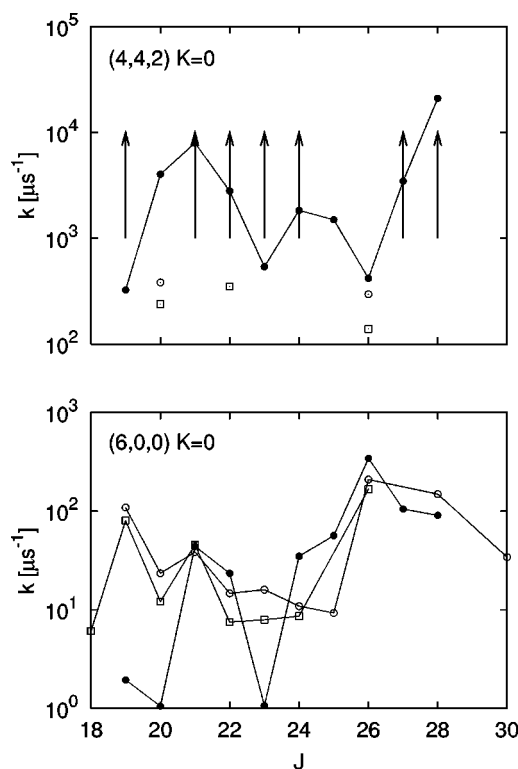


FIG. 1. Comparison of measured and calculated dissociation rates for states (4,4,2) (upper panel) and (6,0,0) (lower panel) for $K=0$. The open circles are the results of Dutton *et al.* (Ref. 3) and the open squares denote the results of Callegari *et al.* (Ref. 2). The arrows in the upper panel indicate that the widths are larger than $10^3 \mu\text{s}^{-1}$ (Ref. 3).

prominent and the variation with J more “regular” (see below).

The mixing between two states can be accidental, if the rotational constants of the two states are drastically different, or it can be more gradual, if the \bar{B} values differ by only a few percent. In the first case, the rate constants show a more random behavior as function of J , while in the second case a more systematic variation, extending over several J values, is expected. An example of a systematic resonance has been analyzed in detail in Ref. 14. The corresponding wave functions clearly revealed, which “dark” state was coupled to the “bright” state. Noteworthy was the observation, that the coupling can be efficient even if the two wave functions have very different nodal structures. In the case investigated in Ref. 14, state (4,2,6) was coupled to a state with zero quanta in the OH mode and many quanta in the dissociation mode. In addition to the overlap of the two wave functions, the energy mismatch is also extremely important. Other examples of mixing effects for HOCl are discussed in Ref. 12.

The fluctuations for the lower J values in Fig. 1 are due to more accidental couplings with vibrational states whose wave functions differ markedly from the (6,0,0) wave function. Analysis of the bound and resonance states near the dissociation threshold^{5,6} has revealed that many of the states with zero or only one quantum of OH stretch have complicated nodal patterns in the other two coordinates, R and γ . Although a large number of these states can be assigned, the assignment is completely different from a normal-mode type assignment. The admixture of such states to (6,0,0) may be very small. However, because they have considerable excitation in the dissociation mode and therefore much larger decay constants than the (6,0,0) level, their effect on the (6,0,0) rate can be large.

The broader maximum at larger J values, on the other hand, must be ascribed to a systematic interaction with state (4,4,2).¹⁻³ For $J=0$ the energies of these two states differ by only 13 cm^{-1} with (4,4,2) being the higher one (Table I). State (4,4,2) has a rotational constant of 0.478 cm^{-1} (experimental value: 0.480 cm^{-1} , Ref. 1), which is only 3% smaller than the constant for (6,0,0). As J increases, the energy of state (6,0,0) rises slightly faster than the energy of (4,4,2) as can be seen in Table I. At $J=26$ the two states are almost degenerate. Inspecting the (6,0,0) wave function confirms that the admixture of (4,4,2) character gradually increases with J and again decreases beyond 26. As a consequence, the width has a pronounced maximum around $J=26$. Actually, for $J=26$ the two states are so strongly mixed, that a clear-cut assignment is ambiguous; the two widths are almost identical. The large contribution of (6,0,0) character to state (4,4,2) explains the minimum around $J=26$. Because either the “bright” or the “dark” state or both states are additionally coupled to other states, the variations of the (6,0,0) rate across the maximum is not smooth, like in other cases where the densities of states are considerably smaller.^{24,25}

The calculated rates are in reasonable agreement with the measured ones; the overall magnitude and the main feature, namely the resonance maximum around $J=26$, are satisfactorily reproduced by the calculations. In order to appreciate the degree of agreement, one has to consider the

tininess of the rates and the related extreme sensitivity to details of the calculations: the PES, the size of the grid, Coriolis coupling, etc. Right at threshold, the energy in the dissociation mode is extremely small (i.e., the de Broglie wavelength is very long) and converging the rate would require a very large grid in R . Thus, the large disagreements for 19 and 20 are not unexpected. For the remaining J values, except for $J=23$, the calculated rate is within a factor of 5 of the experimental result.

The interaction with (4,4,2) around $J=26$ is reasonably well reproduced. This is not surprising, because both levels were included in the correction of the PES in the perturbative inversion scheme.⁹ However, details of this mixing are not correctly described. While the energy mismatch between (6,0,0) and (4,4,2) in the calculations is almost zero at $J=26$, in experiment it is never smaller than 10 cm^{-1} or so (Fig. 10 of Ref. 3).

The experimental method used to determine the dissociation rate does not allow one to measure larger rates. While Callegari *et al.*² quote a detection limit of $0.35 \times 10^3\ \mu\text{s}^{-1}$, Dutton *et al.*³ give an upper limit of rates, which can be unambiguously determined, of $10^3\ \mu\text{s}^{-1}$. For this reason a comparison with the experimental rates for (4,4,2) is restricted (upper panel of Fig. 1). Nevertheless, the order of magnitude is reproduced. According to Dutton *et al.*³ most of the experimental rates are larger than $10^3\ \mu\text{s}^{-1}$, and that is fully consistent with the calculations.

Calculations have been also performed using the TR scheme. The energies are in very good agreement with those in Table I. For (6,0,0) the transition energies calculated with the FD method are systematically $1-2\text{ cm}^{-1}$ larger than those obtained from the TR method; the origin of this mismatch is very likely the different ways by which Coriolis coupling is approximated. While Bowman and co-workers treat overall rotation in an adiabatic approximation,²⁶ in the present study a limited number of K -blocks is directly incorporated. The resonance widths are in the same order of magnitude and show similar fluctuations with J and the interaction with the (4,4,2) state as the ones given in Table I; however, the numbers for the individual J states differ considerably. The rates presented in Table I on the whole agree better with the experimental rates.

B. States (7,0,0)–(9,0,0)

Recently Callegari *et al.*⁴ extended the measurements to $v_1=7$ and 8 and observed a rapid increase of the dissociation rate with each additional OH stretching quantum. Also, the general appearance of the J dependence changes as the degree of OH vibration is increased. The large fluctuations seen for $v_1=6$ are significantly damped and more regular resonance-like structures occur.

We performed calculations in the same way as for (6,0,0) for $v_1=7-9$, with one exception: Coriolis coupling is completely ignored, i.e., only $K=0$ is considered. In view of our limited computer resources the inclusion of three K -blocks would not be practicable. In addition to this purely technical aspect, there are two other arguments why the inclusion of Coriolis coupling may not be as important at these high excitation energies as it is just at the threshold. First, the line-

TABLE II. Calculated resonance energies E and resonance widths Γ for vibrational states (7,0,0), (8,0,0), and (9,0,0).

(7,0,0)			(8,00)			(9,00)		
J	E^a	Γ	J	E	Γ	J	E	Γ
0	21 725.9	4.98(-4) ^b	0	24 173.3	1.9	0	26 431.5	1.08
5	21 741.0	1.3(-3)	2	24 176.5	2.1	2	26 434.2	1.2
10	21 781.3	1.2(-3)	4	24 183.5	2.6	4	26 441.9	6.9(-1)
13	21 817.5	3.7(-3)	6	24 194.6	3.3	6	26 452.5	9.0(-1)
14	21 831.5	3.2(-2)	8	24 210.3	3.8			
15	21 846.6	2.5(-2)	10	24 230.0	2.7			
16	21 862.7	1.6(-2)	12	24 252.6	2.1			
17	21 879.7	3.0(-2)	14	24 280.5	1.0			
18	21 897.6	8.1(-2)	16	24 311.2	5.5(-1)			
19	21 917.6	8.5(-2)	18	24 346.2	1.7(-1)			
20	21 937.5	3.4(-2)	20	24 385.2	3.7(-1)			

^aEnergies and widths in cm^{-1} . The energies are measured with respect to (0,0,0) and $J=0$.

^bNumbers in parentheses indicate powers of 10.

widths are much larger than the (6,0,0) widths and therefore much less sensitive to details of the calculations like errors in the potential or in the dynamical calculations. Second, the effect of Coriolis coupling is essentially a shift of the energies by a few cm^{-1} . This little shift was important for reasonably describing the (6,0,0)/(4,4,2) resonance; remember, both levels were used in the iterative correction of the *ab initio* PES and their energies are perfectly reproduced by the calculations.⁹ That does not apply, however, to the higher members of the OH stretch progression (see below), which were not used for improving the PES. Thus, because the energies of these high levels are not as well reproduced as in the (6,0,0) region, an additional inaccuracy of a few cm^{-1} is not believed to matter much.

The calculated results are summarized in Table II. Because of the limitations of computer time, not every J value has been calculated. $v_1=9$ has been considered in order to check whether the strong increase from $v_2=7$ to 8 is continued beyond $v_2=8$. In each calculation, including $v_1=9$, the ($v_1,0,0$) state could be clearly identified. The experimental transition energies for (7,0,0) and (8,0,0) are⁴ 21 709.2 cm^{-1} and 24 102.1 cm^{-1} , respectively. The deviation of 17 cm^{-1} for $v_1=7$ rises to 71 cm^{-1} for $v_1=8$. Considering that the perturbative correction procedure did take into account only levels up to (6,0,0), these deviations are quite small. The calculated rotational constant is 0.503 cm^{-1} for $v_1=7$ (determined from the energies for $J=0$ and 5) and 0.490 cm^{-1} for $v_1=8$ (determined from the energies for $J=0$ and 2); the experimental values are 0.496 cm^{-1} and 0.493 cm^{-1} .

In full agreement with the experimental data, the widths strongly increase from $v_1=6$ to 7 and again from $v_1=7$ to 8. However, the (9,0,0) widths are of the same overall magnitude as the $v_1=8$ widths, which indicates that the coupling to the continuum does not significantly increase beyond $v_1=8$. A further increase by a factor of 10–50 certainly would have brought the $v_1=9$ width to a range, where it were well above the mean spacing between the levels—in other words, where a state (9,0,0) would not exist any longer because of the supposedly strong coupling between neighboring states. Callegari *et al.* report widths for (7,0,0) in the range of 0.015–0.035 cm^{-1} for $J=13$ –19. For (8,0,0) experimental

widths between 0.5 cm^{-1} and 2.6 cm^{-1} for J between 0 and ~ 30 can be read off Fig. 4 of Ref. 4. In both cases the agreement between theory and experiment is good, as far as the average magnitude is concerned.

In Fig. 2 we depict the rates for (7,0,0) and (8,0,0) as a function of J . The width for $v_1=7$ still shows some sizable fluctuations, which certainly have the same origin as the fluctuations in the case of (6,0,0). A pronounced maximum occurs at $J=19$, which is caused by the tuning in and tuning out of resonance with a nearby state with a shorter lifetime. The wave functions show some admixtures, but a clear assignment of the perturbing state is not possible. Due to the

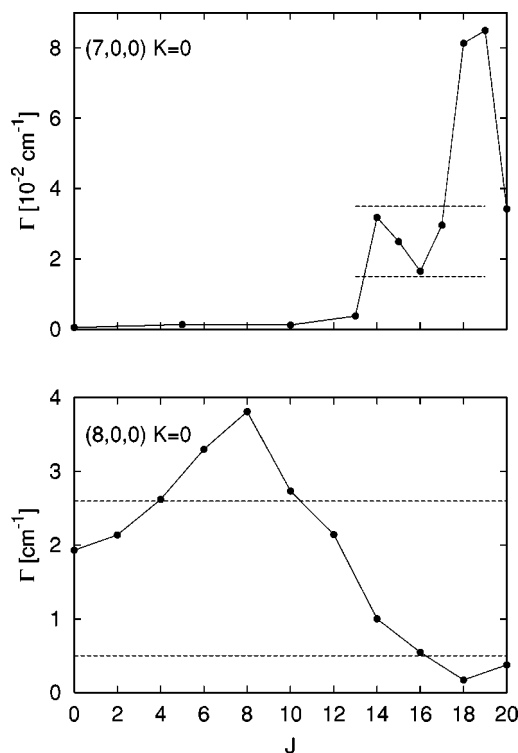


FIG. 2. Calculated resonance widths Γ as function of J for vibrational states (7,0,0) and (8,0,0). The projection quantum number is $K=0$. The horizontal lines indicate the ranges of the measured resonance widths, Ref. 4.

few data points for low J values conclusions about the degree of fluctuations in this range are not possible. A clear resonance structure extending over a large range of J values is obtained for (8,0,0). The experimental (8,0,0) width also shows a broad maximum, however at a slightly higher J value, $J=15$.

Parallel to the present study, Zou *et al.*²⁷ also calculated the resonances for $v_1=7$ and 8, however, only for $J=0$. The potentials employed in the two calculations are the same. The calculated transition energies are 21 725 and 24 172 cm^{-1} and agree very well with the ones given in Table II. The widths are 0.01 and 0.6 cm^{-1} , respectively, and also agree reasonably with the results quoted in Table II.

IV. DISCUSSION

The sharp rise of Γ from (6,0,0) to (8,0,0) is not untypical for a system with very regular intramolecular dynamics with one mode (OH in the case of HOCl) being very weakly coupled to the dissociation mode. Another example is the dissociation of the S_N2 system $\text{Cl}^- \cdots \text{CH}_3\text{Cl}$ recently investigated by Schmatz *et al.*²⁸ It is characterized by exceedingly weak coupling between the fast CH_3Cl intramolecular mode and the slow $\text{Cl}^- \cdots \text{CH}_3$ intermolecular mode. The lower bound of the distribution of resonance widths—determined basically by the overtones of the intramolecular mode—rises by more than seven orders of magnitude from threshold to about 4000 cm^{-1} above threshold. HCO is another molecule which commonly is considered to belong to the weak-coupling case.^{29,30} Nevertheless, the increase of Γ with the CO vibrational quantum number is much more gradual and certainly less rapid than for HOCl (Fig. 9 of Ref. 31).

The reason for the difference in the behaviors of HOCl and the S_N2 system, on the one hand, and HCO, on the other, may be the different degrees of adiabatic separability. In addition to the coupling provided by the PES, the frequency ratios are also relevant. The ratio of the frequency of the internal vibrational mode and the frequency of the dissociation mode is merely ~ 0.75 for HCO, whereas for HOCl it is ~ 5 ; for $\text{Cl}^- \cdots \text{CH}_3\text{Cl}$ the equivalent ratio is even larger, ~ 6 . In other words, a vibrationally adiabatic approximation³² is expected to be much more accurate for HOCl than it is for HCO. In the following we will use the adiabatic picture to qualitatively rationalize the strong increase of Γ for HOCl.

In the adiabatic picture one solves the one-dimensional Schrödinger equation for the fast mode, i.e., the OH stretching mode in the present case for fixed value of the slow mode, R ; the bending angle is fixed at the equilibrium angle of HOCl. In what follows the bending degree of freedom is not considered. This defines the adiabatic energies $\epsilon_{v_1}(R)$ and the adiabatic wave functions $\phi_{v_1}(r;R)$. The one-dimensional energy curves for $v_1=0-9$ are displayed in Fig. 3(a). They are almost parallel to each other, which reflects the high degree of separability of these two degrees of freedom. The energy of, e.g., state (8,0,0) is well approximated by the lowest energy of the potential curve $\epsilon_8(R)$ and the corresponding wave function is approximately given by the product $\phi_8(r;R)\psi_{(8,0)}(R)$, where $\psi_{(8,0)}(R)$ is the wave

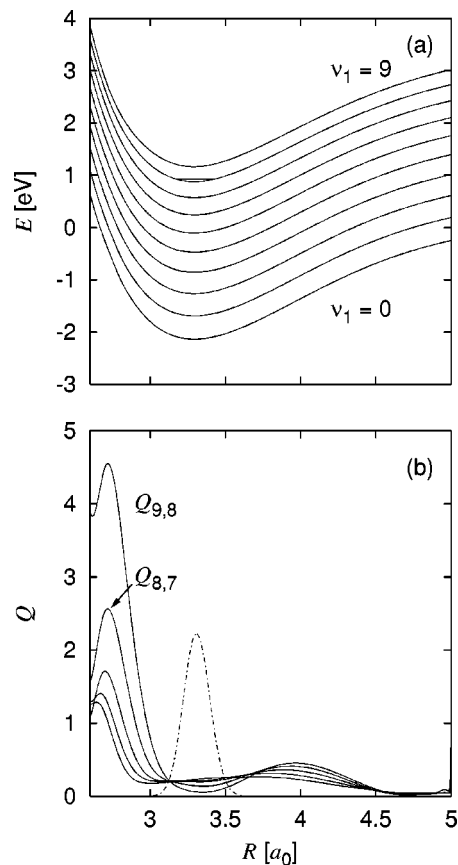


FIG. 3. (a) Vibrationally adiabatic potential curves $\epsilon_{v_1}(R)$ for $v_1=0-9$. The bending angle is fixed at the HOCl equilibrium angle. The horizontal line indicates the adiabatic energy for the lowest state for $v=8$. (b) Nonadiabatic coupling elements Q_{v_1, v'_1} (arbitrary units) for transitions $9 \rightarrow 8$, $8 \rightarrow 7$, etc. The dashed-dotted curve is the wave function for the lowest state for OH vibrational state $v_1=8$.

function of the lowest state in the R mode of vibrational state $v=8$.

In order to dissociate, a state $(v_1, 0, 0)$ must undergo a sequence of nonadiabatic transitions until the $v_1=0$ “tier” is reached. The nonadiabatic transitions are promoted by the matrix elements,³²

$$Q_{v_1, v'_1} \propto \left\langle \phi_{v_1}(r;R) \left| \frac{\partial}{\partial R} \right| \phi_{v'_1}(r;R) \right\rangle_r, \quad (1)$$

where the integration is over r . The matrix elements connecting neighboring states, Q_{v_1, v_1-1} , are shown in Fig. 3(b). The most distinct feature is their steep rising at small distances, in the repulsive branch of the PES. Around the equilibrium and at larger R values the coupling elements are smaller and less R dependent.

The matrix element for a transition from the initial state $(v_1, 0)$ to state (v_1-1, v_3) is given by

$$\langle \psi_{(v_1, 0)} | Q_{v_1, v_1-1} | \psi_{(v_1-1, v_3)} \rangle_R, \quad (2)$$

where integration is over R . The final wave function $\psi_{(v_1-1, v_3)}$ has to be considerably excited in the R coordinate in order that its energy approximately matches the energy of the initial state. As a consequence, the overlap integral Eq. (2) is essentially determined at smaller internuclear dis-

tances, near the inner turning points. At larger distances the final state wave function oscillates and positive and negative parts cancel each other. In other words, the matrix element is mainly determined by the overlap of the inner most maximum of the final state wave function, the small- R branch of the initial wave function and the coupling element Q_{v_1, v_1-1} . However, the coupling element at small distances significantly increases with v_1 and therefore the transition matrix elements are expected to also strongly increase with v_1 . Because a whole cascade of nonadiabatic transitions are required before dissociation is possible, it appears plausible that the resonance width grows approximately exponentially with v_1 —until the transition probability becomes too large for perturbation theory to be valid any longer. For HOCl, this might be the case for $v_1=9$.

The widths show pronounced structures when the rotational quantum number J is varied. These structures are caused by mixings with other resonances, which have considerably broader widths. Changing J tunes this mixing into resonance and out of resonance. Similar features have been seen in calculations for the unimolecular dissociation of HCO (Refs. 25, 33, 34) and the photodissociation of HNO.²⁴ The correct reproduction of these mixing effects requires very precise dynamics calculations and extremely accurate potential energy surfaces. Both, for HOCl and HNO the *ab initio* PESs are not sufficiently accurate. Resonance effects are observed in the calculations, but not at the right places.

As pointed out by Callegari *et al.*,⁴ the more accidental fluctuations are less pronounced in the high energy regime. We observe the same tendency in our calculations. The variation of Γ for $v_1=8$ over a large range of J values is much smoother than for 6 and 7. There are at least two reasons. First, the average width is already so large at these high energies that small perturbations are not so relevant any longer; in addition, the ratio of the widths of the bright state and the perturbing state is expected to be significantly smaller at higher energies than at lower excitations with the consequence that the relative increase is also smaller. The second reason has to do with the density of states, which can serve as perturbing states. Roughly speaking, one can define three classes of resonance states: very narrow ones, like (8,0,0), for example, very broad ones, and resonance states with medium size widths, so-called “doorway” states. The very broad resonances have many quanta of excitation in the dissociation mode; they have no distinct identity and form the “background.” The coupling of the narrow resonances to the background changes in a gradual, not specific manner with energy and if no “doorway” state is in the vicinity, Γ varies very smoothly with e.g., J . Illustrative examples can be found in Ref. 24. The coupling to the “doorway” states is more specific; it depends on the energy mismatch and the particular nodal structures of the wave functions. Mixing with these states leads to the resonancelike structures of the width. With increasing energy, the average width gradually increases, the overlap of resonances becomes more severe, and the density of “doorway states” decreases.⁴ As a consequence, the variation of Γ with J becomes smoother.

V. SUMMARY

(1) Large-scale dynamics calculations have been performed for studying the unimolecular dissociation of the pure OH stretching states, $(v_1, 0, 0)$, of HOCl in the ground electronic state. The calculations use filter diagonalization and an absorbing potential. An accurate potential energy surface has been employed.

(2) The average width increases by four orders of magnitude from $v_1=6$ through 9. This strong increase is rationalized in terms of a vibrationally adiabatic model and the shape of the nonadiabatic coupling elements. It seems to be typical for molecules in which one degree of freedom is very weakly coupled to the other modes. The weak coupling is the consequence of the shape of the potential energy surface and the large mismatch between the three frequencies.

(3) The resonance widths show pronounced structures as function of the total angular momentum quantum number J . These structures are due to mixings with nearby “doorway” states. Because the rotational constants depend on the vibrational states, the energy gap between the bright and the dark states is tuned as J is varied. The structures become more regular and systematic with higher energies, which, probably, is the consequence of the lower density of “doorway” states in the high-energy regime.

(4) The agreement with the experimental resonance widths is satisfactory. The average width, averaged with respect to J , is very well reproduced by the calculations. The more distinct resonance-like structures are only qualitatively described: They are seen in the calculations, but not at the right J values, except for the (6,0,0)/(4,4,2) resonance around $J\sim 26$. The correct description of the mixings between different states requires a higher accuracy of the potential energy surface. Nevertheless, in view of the detailed experimental data, the potential energy surface calculations, and the various dynamical studies one can consider the unimolecular dissociation to be basically understood.

ACKNOWLEDGMENTS

Financial support by the Deutsche Forschungsgemeinschaft through the Sonderforschungsbereich 357 “Molekulare Mechanismen Unimolekularer Reaktionen” and the Fonds der Chemischen Industrie is gratefully acknowledged. One of the authors (R.S.) enjoyed many fruitful discussions with S. Yu. Grebenshchikov and T. R. Rizzo on the dissociation of HOCl. J.M.B. thanks the U.S. Department of Energy (DE-FG02-97ER14782) for financial support and V.A.M. acknowledges support of the National Science Foundation (CHE-0108823). K.A.P. thanks the National Science Foundation (CHE-9501262) and the U.S. Department of Energy (DE-AC06-76RLO 1830) for financial support. All calculations have been performed on the CRAY T3E parallel computer of the Gesellschaft für Wissenschaftliche Datenverarbeitung Göttingen (GWDG).

¹A. Callegari, J. Rebstein, J. S. Muentner, R. Jost, and T. R. Rizzo, *J. Chem. Phys.* **111**, 123 (1999).

²A. Callegari, J. Rebstein, R. Jost, and T. R. Rizzo, *J. Chem. Phys.* **111**, 7359 (1999).

³G. Dutton, R. J. Barnes, and A. Sinha, *J. Chem. Phys.* **111**, 4976 (1999).

- ⁴A. Callegari, R. Schmied, P. Theulé, J. Rebstein, and T. R. Rizzo, *Phys. Chem. Chem. Phys.* **3**, 2245 (2001).
- ⁵R. Jost, M. Joyeux, S. Skokov, and J. M. Bowman, *J. Chem. Phys.* **111**, 6807 (1999).
- ⁶J. Weiß, J. Hauschildt, S. Yu. Grebenshchikov, R. Düren, R. Schinke, J. Koput, S. Stamatiadis, and S. C. Farantos, *J. Chem. Phys.* **112**, 77 (2000).
- ⁷S. Skokov, K. A. Peterson, and J. M. Bowman, *J. Chem. Phys.* **109**, 2662 (1998).
- ⁸K. A. Peterson, S. Skokov, and J. M. Bowman, *J. Chem. Phys.* **111**, 7446 (1999).
- ⁹S. Skokov, K. A. Peterson, and J. M. Bowman, *Chem. Phys. Lett.* **312**, 494 (1999).
- ¹⁰S. Skokov, J. Qi, J. M. Bowman, C.-Y. Yang, S. K. Gray, K. A. Peterson, and V. A. Mandelshtam, *J. Chem. Phys.* **109**, 10273 (1998).
- ¹¹S. Skokov, J. M. Bowman, and V. A. Mandelshtam, *Phys. Chem. Chem. Phys.* **1**, 1279 (1999).
- ¹²S. Skokov and J. M. Bowman, *J. Chem. Phys.* **110**, 9789 (1999).
- ¹³J. Hauschildt, J. Weiß, C. Beck, S. Yu. Grebenshchikov, R. Düren, R. Schinke, and J. Koput, *Chem. Phys. Lett.* **300**, 569 (1999).
- ¹⁴J. Hauschildt, J. Weiß, and R. Schinke, *Z. Phys. Chem. (Munich)* **214**, 609 (2000).
- ¹⁵M. R. Wall and D. Neuhauser, *J. Chem. Phys.* **102**, 8011 (1995).
- ¹⁶V. A. Mandelshtam and H. S. Taylor, *J. Chem. Phys.* **103**, 2903 (1995).
- ¹⁷V. A. Mandelshtam, T. P. Grozdanov, and H. S. Taylor, *J. Chem. Phys.* **103**, 10074 (1995).
- ¹⁸T. P. Grozdanov, V. A. Mandelshtam, and H. S. Taylor, *J. Chem. Phys.* **103**, 7990 (1995).
- ¹⁹R. Kosloff, *J. Phys. Chem.* **92**, 2087 (1988).
- ²⁰B. Hartke, R. Kosloff, and S. Ruhman, *Chem. Phys. Lett.* **158**, 238 (1989).
- ²¹Y. Huang, W. Zhu, D. J. Kouri, and D. K. Hoffman, *Chem. Phys. Lett.* **206**, 96 (1993).
- ²²J. Echave and D. C. Clary, *Chem. Phys. Lett.* **190**, 225 (1992).
- ²³Z. Bačić and J. C. Light, *Annu. Rev. Phys. Chem.* **40**, 469 (1989).
- ²⁴J. Weiß and R. Schinke, *J. Chem. Phys.* **115**, 3173 (2001).
- ²⁵U. Brandt-Pollmann, J. Weiß, and R. Schinke, *J. Chem. Phys.* **115**, 8876 (2001), preceding article.
- ²⁶J. M. Bowman, *Chem. Phys. Lett.* **217**, 36 (1994).
- ²⁷S. Zou, S. Skokov, and J. M. Bowman, *Chem. Phys. Lett.* **339**, 290 (2001).
- ²⁸S. Schmatz, P. Botschwina, J. Hauschildt, and R. Schinke, *J. Chem. Phys.* **114**, 5233 (2001).
- ²⁹D. Wang and J. M. Bowman, *Chem. Phys. Lett.* **235**, 277 (1995).
- ³⁰R. Schinke, C. Beck, S. Yu. Grebenshchikov, and H.-M. Keller, *Ber. Bunsenges. Phys. Chem.* **102**, 593 (1998).
- ³¹H.-M. Keller, H. Flöthmann, A. J. Dobbyn, R. Schinke, H.-J. Werner, C. Bauer, and P. Rosmus, *J. Chem. Phys.* **105**, 4983 (1996).
- ³²R. Schinke, *Photodissociation Dynamics* (Cambridge University Press, Cambridge, 1993).
- ³³J. Qi and J. M. Bowman, *J. Chem. Phys.* **105**, 9884 (1996).
- ³⁴C.-Y. Yang and S. K. Gray, *J. Chem. Phys.* **107**, 7773 (1997).